ELSEVIER

Journal of Alloys and Compounds 356–357 (2003) 579–583

Journal of ALLOYS AND COMPOUNDS

www.elsevier.com/locate/jallcom

Role of Zr and Ga additions on the hydrogen process of Nd–Fe–B magnets

P. de Rango[a,b,*], S. Rivoirard[b], A. Traverse[c], D. Fruchart[a,b], F.N. Genin[a]

[a] *Laboratoire de Cristallographie du CNRS, BP 166, 38042 Grenoble Cedex 9, France*
[b] *Consortium de Recherche pour l'Etudes de Technologies Avancées, BP 166, 38042 Grenoble Cedex 9, France*
[c] *Laboratoire pour l'Utilisation du Rayonnement Synchrotron, Bat 405D, Université Paris-Sud, 91000 Orsay Cedex, France*

Received 27 August 2002; accepted 25 October 2002

Abstract

Highly coercive Nd–Fe–B powders for bonded magnets have been successfully produced applying hydrogen processes such as hydrogen decrepitation (HD) or hydrogen–disproportionation–dehydrogenation–recombination (HDDR). XAFS experiments were performed in order to localise the extra elements. Zr addition results in the formation of fine ZrB_2 precipitates, whereas Ga substitutes the Fe(4c) site in the $Nd_2Fe_{14}B$ structure. Systematic analyses of the hydrogen disproportionation kinetics by thermomagnetic measurements have permitted to point out different regimes of reactivity depending on both the used extra elements and the temperature. It is found that the ZrB_2 precipitates act as barriers limiting hydrogen diffusion at the crystallites boundaries and lead to uncompleted disproportionation reactions. Then the $Nd_2Fe_{14}B$ remaining particles act as nucleation centres that can be used to induce oriented growth during the recombination step.

Keywords: Permanent magnets; EXAFS; Solid–gas reaction

1. Introduction

With the development of bonded magnets, impulses are done to optimise powders with high level extrinsic properties. In these powders, the coercive force is directly related to the microstructure. To avoid the propagation of the domain walls, the size of the elementary crystallites must be controlled as well as the distribution of the minor intergranular Nd-rich phase. Furthermore, if the grains are textured, i.e. with crystallites oriented along a common direction, the inductive force of the resulting magnet can be magnified up to 2.

Two processes involving hydrogenation of bulk Nd–Fe–B alloys have been developed to produce highly coercive and anisotropic powders. The hydrogen decrepitation (HD), a low temperature process, applies on starting anisotropic and coercive bulk materials [1,2]. On the contrary, the hydrogen-disproportionation desorption-recombination (HDDR) process, first reported by Takeshita and Nakayama [3], applies directly on a standard alloy. It consists in the disproportionation of the starting alloy under a hydrogen atmosphere above 600 °C, according to the reaction (1):

$$Nd_2Fe_{14}B + xH_2 \rightarrow 2NdH_x + \alpha\text{-}Fe + Fe_2B \quad (1)$$

followed by a recombination reaction to form an improved microstructure after desorption using a vacuum heat treatment typically around 850 °C. The transformation of the initial coarse grains into very fine grains is responsible for the high coercivity, but the resulting powders are isotropic. Additions of small amounts of extra elements (Zr, Nb, Ga, Co, etc.) have been reported to improve coercitivity and/or to induce an oriented growth of the elementary crystallites during the recombination step [4,5]. Because of their different roles, it appeared of first importance to carefully localise these extra elements. This was achieved for Zr and Ga by performing EXAFS experiments on doped $Nd_2Fe_{14}B$ alloys. Systematic analyses of the hydrogen-disproportionation kinetics by thermomagnetic measurements led to a better understanding of the role of Zr in inducing anisotropy.

*Corresponding author. Fax: +33-4-7688-1280.
E-mail address: derango@grenoble.cnrs.fr (P. de Rango).

0925-8388/02/$ – see front matter © 2002 Published by Elsevier B.V.
doi:10.1016/S0925-8388(02)01280-X

2. Experiment

Alloys of chemical compositions $Nd_{11.76}Fe_{82.36}B_{5.88}$ (stoichiometric $Nd_2Fe_{14}B$), $Nd_{11.75}Fe_{82.25}B_{5.85}Zr_{0.15}$, $Nd_{11.7}Fe_{81.8}B_{5.8}Zr_{0.7}$, and $Nd_{11.5}Fe_{80.2}B_{5.7}Ga_{2.6}$ were prepared by induction melting under argon atmosphere. These alloys were annealed at 1000 °C during 6 h for homogenisation. They were crushed into powders, then sieved to 200 μm. The mean grain size as controlled using a laser granulometer was 157±5 μm for the undoped and the Zr-doped (0.7 at.%) powders. The X-ray diffraction patterns recorded on these specimens reveal $Nd_2Fe_{14}B$ single phase materials.

XAFS experiments were carried out at LURE (France) in transmission mode, using a channel-cut monochromator, at 77 K, at the K-edge of Zr and Ga. The data treatment was achieved in the usual way using the Michalowicz code [6]. Ab initio calculations of the oscillations were also performed with the FEFF code [7]. The Fourier Transforms (FT) were calculated in the same way as for the experimental ones for comparison purposes.

Thermomagnetic measurements were performed using a home-made torque allowing us to record the magnetic characteristics of a sample under gas reaction. The powder was placed under a continuous hydrogen flow and the applied magnetic field was close to 2 kOe. Samples were heated at a rate of 10 °C/min up to a plateau between 600 and 750 °C, and then cooled down at 10 °C/min.

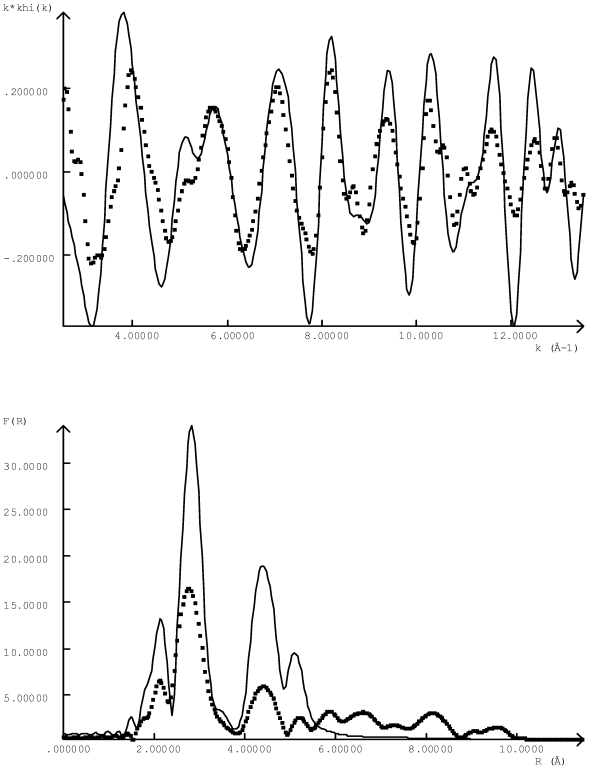

Fig. 1. XAFS spectra (a) and Fourier Transforms (b) at the Zr K-edge observed for Zr = 0.7 at.% (dashed lines) and calculated for ZrB_2 phase (full lines).

3. Localisation of the additives

The XAFS spectra and FT obtained from the oscillations taken at the Zr K-edge on the $Nd_{11.7}Fe_{81.8}B_{5.8}Zr_{0.7}$ alloy are presented Fig. 1. We calculated XAFS spectra and FT, (i) for Zr located on each of the six possible Fe sites, the two Nd and the B sites in the $Nd_2Fe_{14}B$ structure, (ii) for Zr located in the ZrB_2 phase (space group *P6/mmm*, $a = 3.168$ Å and $c = 3.530$ Å). Each of the FT calculated for Zr substituting one of the sites in $Nd_2Fe_{14}B$ does not fit the experimental data. The XAFS spectra and FT calculated for ZrB_2 phase are the only ones that compare well with the experimental results (Fig. 1). Matzinger et al. have shown that the boride exists in magnet materials as platelet-like ZrB_2 precipitates within the Nd-rich intergranular region [8].

XAFS measurements were performed at the Ga K-edge on the $Nd_{11.5}Fe_{80.2}B_{5.7}Ga_{2.6}$ alloy. XAFS spectra and FT were calculated for each of the six Fe sites, the two Nd sites and the B site of $Nd_2Fe_{14}B$. Only the ones calculated for Ga substituting the Fe(4c) site in $Nd_2Fe_{14}B$ fit the observed ones (Fig. 2), indicating that most of the Ga atoms occupy this site. This result is in good agreement with XAFS measurements carried out by Ashfaq et al. on a $Nd_{13.0}Fe_{68.2}Co_{10.8}Ga_{1.0}Zr_{0.1}B_{6.9}$ alloy [9].

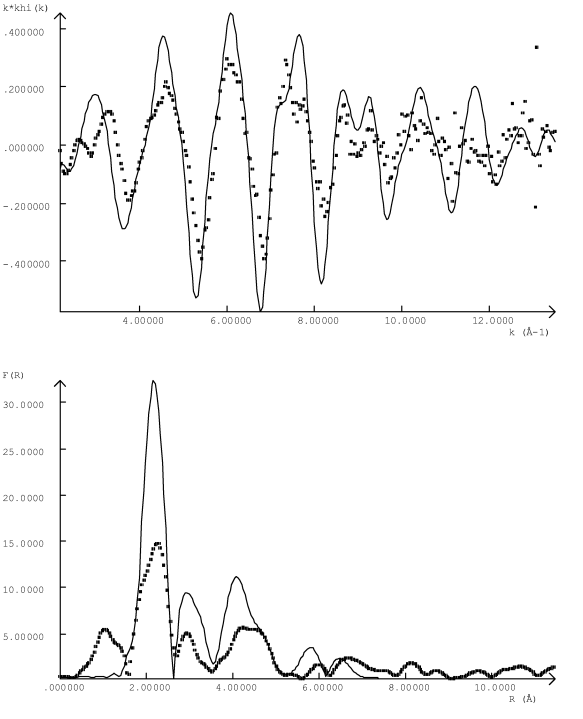

Fig. 2. XAFS spectra (a) and FT (b) at the Ga K-edge observed for Ga = 2.6 at.% (dashed lines) and calculated for Ga substituting to the Fe(4c) site in $Nd_2Fe_{14}B$ (full lines).

4. Thermomagnetic analyses of the disproportionation reaction

4.1. Undoped $Nd_2Fe_{14}B$

The trace diagram recorded during the disproportionation process of a stoichiometric $Nd_2Fe_{14}B$ powder is presented in Fig. 3a. During heating a slight increase in the magnetisation due to the hydrogenation of the $Nd_2Fe_{14}B$ phase (step 1) is observed as well as a sharp decrease at the Curie temperature (T_C) of the hydrogenated $Nd_2Fe_{14}BH_x$ phase (step 2). Up to 625 °C, no further variation of magnetisation is observed. An increase of magnetisation takes place during the plateau at 625 °C (step 3) due to the formation of free iron, associated with the $Nd_2Fe_{14}BH_x$ disproportionation. A complete disproportionation reaction is achieved if the rest time at the plateau is long enough. However, if the sample is cooled down before completion of this process, the resulting specimen is a mixture of disproportionated and nondisproportionated particles. Besides, the increase in magnetisation observed at lower temperature is related to the remains of hydrogenated $Nd_2Fe_{14}BH_x$ as detected from its Curie temperature (step 4). Thus, we are able to estimate the rate of disproportionation at the end of the thermal treatment from the height of the transitions at T_C before and after reaction.

At moderate temperatures, the kinetics of the disproportionation reaction is low enough and the amount of $Nd_2Fe_{14}BH_x$ disproportionated during the increase of temperature can be neglected. Then, the increase of magnetisation corresponding to free iron formation can be normalized so that the beginning of the disproportionation reaction corresponds to the beginning of the plateau ($m=0$ at $t=0$) and that at the end of the plateau, m is equal to the rate of disproportionation deduced from the heights at T_C ($m=1$ if reaction is over). Then, the normalised magnetization m plotted versus time t allows us to follow the rate of the reaction all along the plateau (Fig. 3b).

The experimental data were analysed in the light of known propagation mechanisms for a solid reaction across spherical particles of radius r [10,11]. Two regimes have been observed on undoped $Nd_2Fe_{14}B$ alloys:

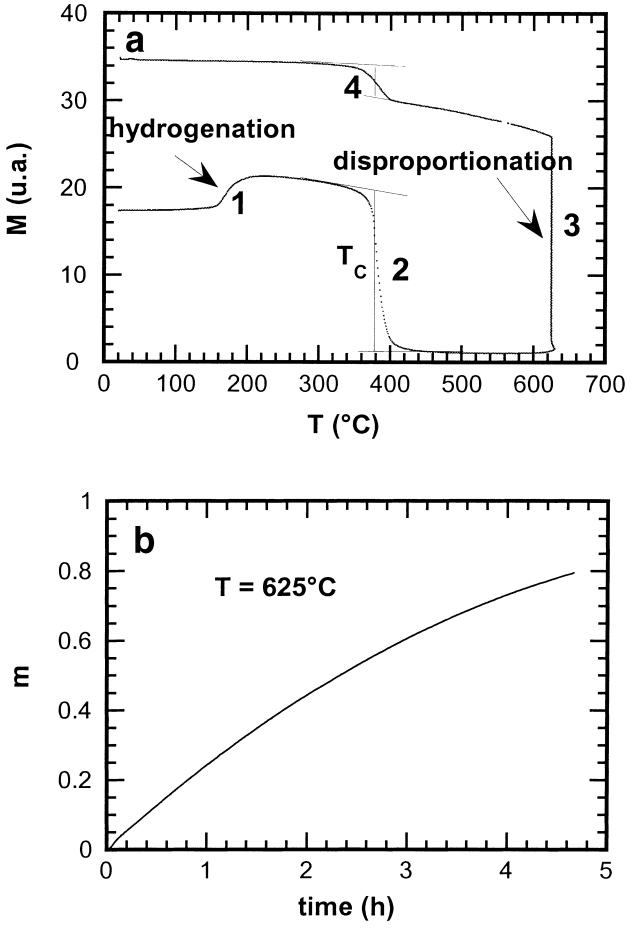

Fig. 3. (a) Variation of magnetisation versus temperature during a disproportionation reaction under hydrogen flow for a stoichiometric $Nd_2Fe_{14}B$ compound, (b) disproportionate rate versus time, during the 5 h stage at 625 °C.

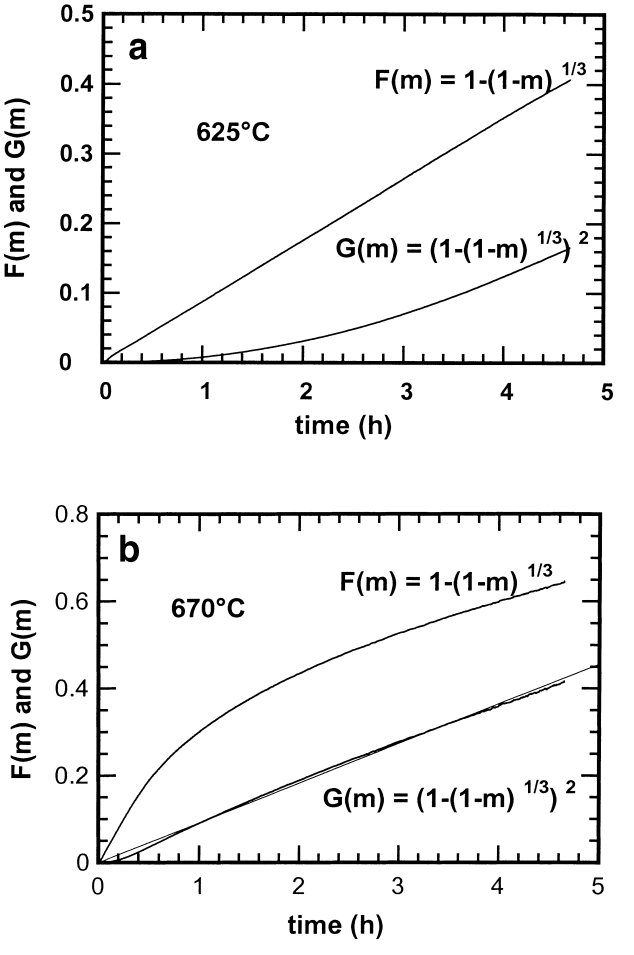

Fig. 4. $F(m)$ and $G(m)$ functions at 625 °C (a) and 670 °C (b) for a $Nd_2Fe_{14}B$ stoichiometric alloy.

- at moderate temperature ($T \leq 625$ °C), the disproportion process corresponds to an interface progression mechanism having a constant speed u. As seen in Fig. 4a for $T = 625$ °C, the rate of the reaction follows the equation: $F(m) = 1 - (1 - m)^{1/3} = (u/r) \cdot t$;
- at higher temperatures ($T \geq 650$ °C), the limiting factor becomes the hydrogen diffusion through the decomposed matter. As reported on Fig. 4b for $T = 670$ °C, the disproportion reaction is of Jander type: $G(m) = (1 - (1 - m)^{1/3})^2 = (k/r^2) \cdot t$.

The diffusion constant k is of Arrhenius type $k(T) = k_0 \exp(-E_a/RT)$, E_a being the activation energy and R the ideal gas constant.

This change of behavior should be explained considering the work of Yi et al. [12], who have observed that the decrepitation of the alloy does not take place if the hydrogen is applied above 650 °C. Below this temperature, porosity and voids due to cracks induced inside the disproportionated layer allow the access of the hydrogen gas directly onto the front of the reaction. At higher temperature, a bulk diffusion process takes place quite homogeneously in the materials.

4.2. Zirconium-doped $Nd_2Fe_{14}B$

As observed in Fig. 5, small amounts of zirconium (0.15–0.7 at.%) induce a very important decrease of the disproportionation kinetics. However, by increasing the temperature and/or the time duration of the reaction, a complete disproportionation of the $Nd_2Fe_{14}B$ phase was achieved: the T_C of $Nd_2Fe_{14}B$ is no longer detectable on cooling. With 0.7 at.% of Zr, the disproportionation obeys a Jander law in the whole temperature range, including temperatures below 625 °C (Fig. 6a). The disproportionate rate reported for $T = 740$ °C shows a very good agreement obtained all over the reaction from the Jander law (Fig. 6b).

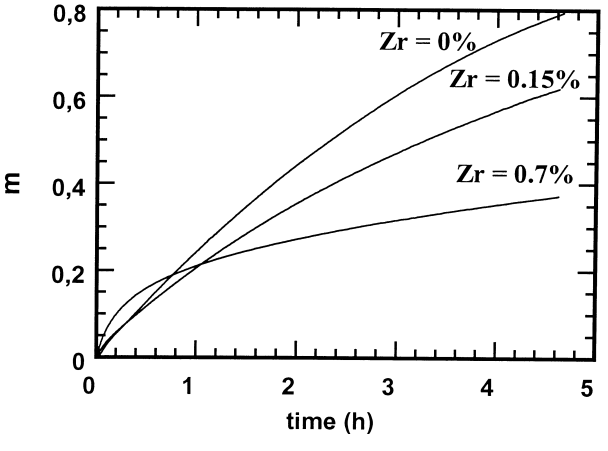

Fig. 5. Variation of the disproportionate rate at 625 °C for increasing amounts of Zr.

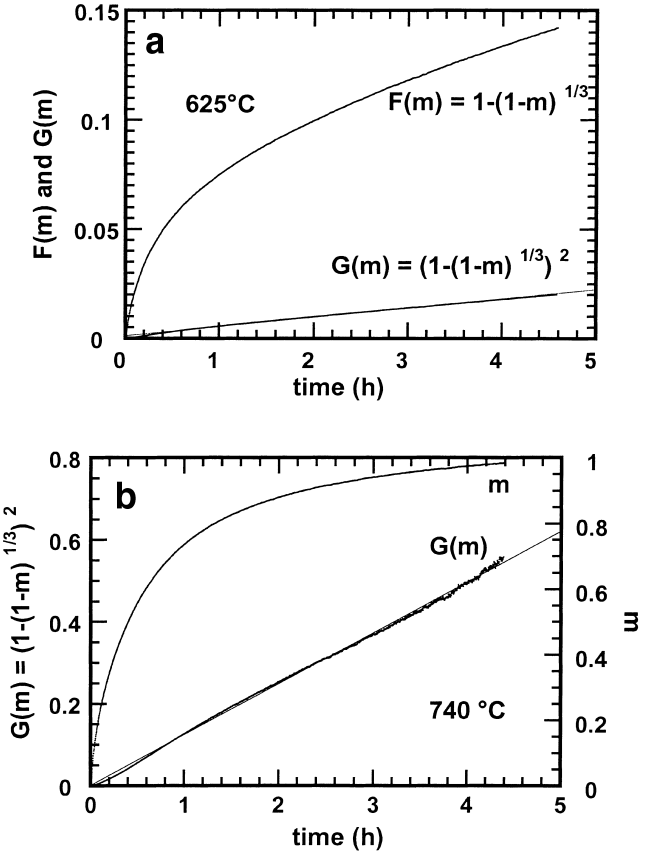

Fig. 6. (a) $F(m)$ and $G(m)$ functions for a $Nd_2Fe_{14}B$ doped Zr alloy at 625 °C and (b) disproportionate rate and $G(m)$ at $T = 740$ °C.

As expected from an Arrhenius feature, a linear behavior of the $\ln(k/r^2)$ experimental data versus $1/T$ is observed, both for the undoped and the Zr = 0.7 at.% compounds (Fig. 7). The activation energies deduced from these data are, respectively, $E_a = 335$ kJ/mol for the undoped decomposed matter and $(E_a)_{Zr} = 228$ kJ/mol for Zr = 0.7 at.%. The impact of Zr addition on k_0/r^2 is much more important. According to the values of the mean grain sizes as determined from laser granulometry, the diffusion

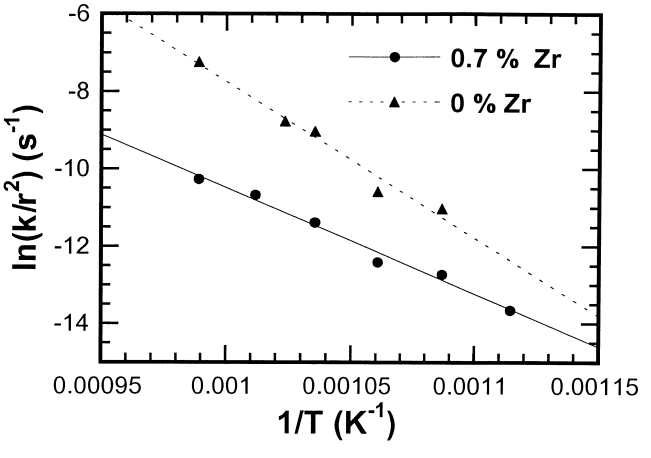

Fig. 7. (k/r^2) parameters, for a stoichiometric $Nd_2Fe_{14}B$ alloy and for Zr = 0.7 at.%, respectively.

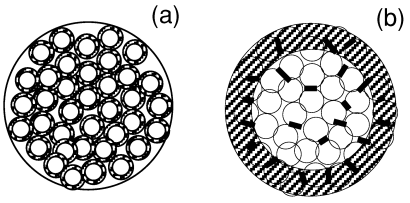

Fig. 8. Two scales of reaction (a) with intergranular hydrogen diffusion for an undoped alloy, (b) without intergranular hydrogen diffusion for ZrB_2 platelets containing alloy.

coefficients are, respectively, $k_0 = 3.7 \times 10^6$ m^2/s for the undoped decomposed matter and $(k_0)_{Zr} = 0.56$ m^2/s for (0.7) doped sample. Nevertheless, the size of the elementary crystallites deduced from the width of the X-ray diffraction peaks [13], are close to 70 and 60 nm, respectively, for the undoped and the Zr = 0.7 at.% samples. If, for the undoped sample, we take into account the size of the elementary crystallites instead of the powder grain size, we obtain $k_0 = 0.72$ m^2/s, which is of the same order of magnitude as the diffusion coefficient previously obtained for the 0.7 at.% Zr-doped sample. In the Zr-free sample, hydrogen diffusion at the crystallites boundaries is much faster than in the intra-granular region, so that it is necessary to take into account the size of the elementary crystallites as seen in Fig. 8a. Few zirconium addition induces the formation of ZrB_2 precipitates which act as barriers limiting hydrogen diffusion within the crystallites boundaries (Fig. 8b).

4.3. Gallium-doped $Nd_2Fe_{14}B$

The disproportionation rate was measured at several temperatures for Ga = 2.6 at.%. Generally speaking, the observed behavior is the same as for undoped $Nd_2Fe_{14}B$. Below 650 °C the reaction is still controlled by an interface progression wall at a constant speed, as seen in Fig. 9. When Ga is substituted into $Nd_2Fe_{14}B$, it does not induce barriers limiting hydrogen diffusion as it is observed for Zr. Moreover, the kinetics slightly increases with Ga addition. Then the Ga containing $Nd_2Fe_{14}B$ phase is not stabilised against hydrogen disproportionation.

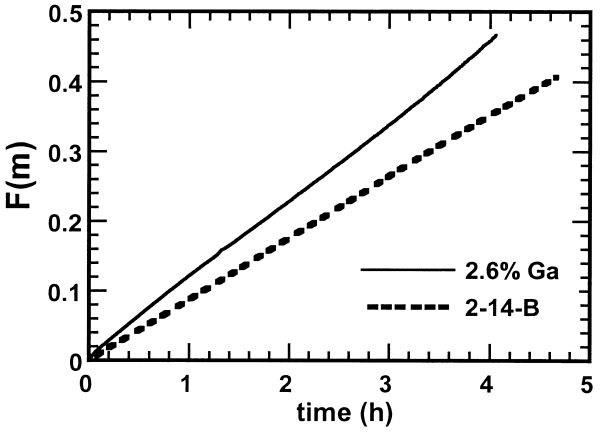

Fig. 9. $F(m)$ at 625 °C, for a stoichiometric $Nd_2Fe_{14}B$ compound and for Ga = 2.6 at.%.

5. Discussion

Thermal treatments currently applied for the disproportionation are typically of 1 h at about 740 °C. At this temperature, the complete disproportionation of the stoichiometric $Nd_2Fe_{14}B$ powder is achieved in 0.38 h, whereas it takes more than 7 h for the 0.7 at.% Zr-doped powder. Moreover, as observed in Fig. 6b, the hydrogen diffusion mechanism induces a very slow decrease of the disproportionation rate at the end of the reaction. Then, the addition of Zr leads to an incomplete disproportionation reaction with the production of nanoscaled $Nd_2Fe_{14}B$ particles in the disproportionated mixture. Thanks to the crystallographic orientation of these particles relative to the original $Nd_2Fe_{14}B$, they can act as nuclei to induce an oriented growth during the recombination step.

Thus, the memory site effect of the Zr on oriented growth can be explained in terms of kinetics of the disproportionation reaction, an incomplete disproportionation reaction being necessary to preserve extra fine particles of non-decomposed $Nd_2Fe_{14}B$. We previously observed similar mechanisms to occur in samples without any Zr [14]. Since in this scenario the induced magnetic anisotropy highly depends on the conditions selected to apply hydrogen, it remained somewhat puzzling how to optimise the HDDR process.

Gallium substituted to Fe(4c) site in the $Nd_2Fe_{14}B$ structure. As far as the disproportionation rate slightly increased with Ga addition, the induced anisotropy cannot be explained in terms of a partial disproportionation reaction and the role of Ga remains unclear.

References

[1] D. Fruchart et al., Patent EP no. EP 85 401 230.9 (1985).
[2] D. Fruchart et al., Patent no. EP 90 06-206 (1991).
[3] T. Takeshita, R. Nakayama, in: 11th Workshop on Rare Earth Magnets and their Applications, Pittsburgh (USA), 1990, p. 49.
[4] R. Nakayama, T. Takeshita, J. Alloys Comp. 193 (1–2) (1993) 259.
[5] T. Tomida, N. Sano, K. Hanafusa, H. Tomizawa, S. Hirosawa, Acta Mater. 47 (1999) 875–885.
[6] A. Michalowicz, J. Phys. IV, France 7 C2, 235 (1997) 235-236.
[7] J.J. Rehr, J. Mustre, S.I. Zabinsky, R.C. Albers, J. Am. Chem. Soc. 113 (1991) 5135.
[8] M. Matzinger, J. Fidler, A. Fujita, I.R. Harris, J. Magn. Magn. Mater. 157/158 (1996) 54.
[9] A. Ashfaq, M. Matsuura, N. Ikuta, M. Sakurai, J. Appl. Phys. 85 (1999) 5681.
[10] G. Valensi, CR Acad. Sci. 202 (4) (1950) 309.
[11] W. Jander, Z. Anorg. Allg. Chem. 163 (1) (1927) 1–30.
[12] G. Yi, J.P. Chapman, D.N. Brown, I.R. Harris, J. Magn. Magn. Mater. 220 (2000) 115.
[13] P. Scherrer, Nachr. Ges. Wiss. Göttingen 98 (1918).
[14] S. Liesert, P. de Rango, J.L. Soubeyroux, D. Fruchart, R. Perrier de la Bâthie, J. Magn. Magn. Mater. 157–158 (1996) 57.